Received: 6 September 2019 | Revised: 27 December 2019 | Accepted: 22 January 2020

DOI: 10.1002/app.49057

ARTICLE

Applied Polymer Science WILEY

Fabrication and characterization of silane-functionalized Na-bentonite polysulfone/polyethylenimine nanocomposite membranes for dye removal

Seda Saki[1] | **Dilek Senol-Arslan**[2] | **Nigmet Uzal**[3]

[1]Department of Materials Science and Mechanical Engineering, Abdullah Gul University, Kayseri, Turkey

[2]Department of Material Science and Nanotechnology Engineering, Abdullah Gul University, Kayseri, Turkey

[3]Department of Civil Engineering, Abdullah Gul University, Kayseri, Turkey

Correspondence
Nigmet Uzal, Department of Civil Engineering, Abdullah Gul University, Kayseri 38380, Turkey.
Email: nigmet.uzal@agu.edu.tr

Abstract

In this study, tetraethoxysilane (TEOS)-functionalized Na-bentonite incorporated into polysulfone/polyethylenimine (PSF/PEI) membranes were fabricated by phase inversion method for the efficient removal of methylene blue dye. For the preparation of PSF/PEI nanocomposite membranes, silane-functionalized Na-bentonite and pure Na-bentonite were used at three different concentrations (0.5, 1, and 2 wt%). The prepared membranes were characterized by Fourier transform infrared spectroscopy, scanning electron microscopy, atomic force microscopy, porosity, hydrophilicity, and water permeability measurements. Antifouling behaviors and methylene blue dye rejections of the PSF/PEI nanocomposite membranes were also tested. The obtained results showed that the addition of pure Na-bentonite and silane-functionalized Na-bentonite both increased the water permeability of the membranes. The PSF/PEI membrane containing 2 wt% silane-functionalized Na-bentonite showed the highest water flux of 105 L m^{-2} h^{-1}, while the lowest water flux of 1.2 L m^{-2} h^{-1} was recorded for pure PSF membrane. Filtration results demonstrated that the antifouling capacity was significantly increased due to the negatively charged surface of the newly generated silane-functionalized Na-bentonite PSF/PEI membranes. In summary, TEOS-functionalized Na-bentonite can be used to fabricate PSF/PEI nanocomposite membranes with effective filtration ability, antifouling capacity with lower decay ratio, higher flux recovery ratio, and 99% methylene blue dye removal performance.

KEYWORDS

Clay, Coatings, Membranes

1 | INTRODUCTION

The textile, dye manufacturing, paper, and plastic industries use large quantities of dyes. The disposal of these dyes into the environment is a major concern. Most of the dyes used in these industries are stable, resistible, and long-term water pollutants.[1] Therefore, the discharge of dyes in wastewater is undesirable and many countries have now introduced more stringent discharge standards and increased regulatory measures.[2,3] Membrane technology has been considered a promising solution for the management of colored wastewaters due to its high

removal efficiency, easy operation, and small footprint. Ong et al.[4] operated lab-scale and pilot-scale reactors to evaluate the performance of membranes under various operating conditions and reported membrane performance of more than 90% rejection for different dyes.[5]

The choice of suitable membrane technologies for the treatment of industrial wastewaters depends on both the membrane material and the composition of the wastewater, which directly affect the membrane performance.[6] Although, commercial membranes have been used in colored wastewater treatment, their high cost and higher fouling tendency have resulted in short service life.

To improve the lifetime and hydrophilicity of membranes, the use of hydrophilic polymers and inorganic nanomaterials in the membrane matrix has been extensively adopted to increase the hydrophilicity and antifouling capacity of membranes.[7,8] There has been considerable interest in using functional nanoparticles as additives to enhance the properties of nanocomposite membranes.[9] Although many kinds of nanomaterials have been applied in the fabrication of polymeric nanocomposites, clay minerals have gained widespread scientific and technological acceptance due to their low cost, eco-friendliness, and availability.[10] Clay minerals enhance the permeation capability of membranes by managing the macrostructure and improving the small pore formation, hydrophilicity, porosity, and antifouling properties.[6] Na-bentonite is one of the important clay minerals with excellent physicochemical properties such as higher cation exchange capacity, better dispersibility, and better higher surface area.[11,12]

Previous studies have shown that silane functionalization of nanomaterials could increase the interaction and compatibility between functionalized nanoparticles and the polymer matrix and improve the transport properties of membranes.[13] Xu et al.[14] reported that the addition of silane-functionalized graphene oxide in poly(vinylidene fluoride) (PVDF) membranes increased permeability and rejection. The lowest contact angle and the highest membrane flux values were obtained for the 1 wt% of silane-functionalized graphene nanoparticle incorporated membranes.[14] In the study by Zeng et.al., novel PVDF nanofiltration membranes were prepared by blending with various concentrations of halloysite nanotubes (HNTs) for dye and heavy metal removal. The results showed that the hydrophilicity, dye rejection, heavy metal rejection, and adsorption capacity of PVDF/silane functionalized HNTs were enhanced significantly.[13] Besides these functionalization methods, silica nanoparticle was silanized to introduce free thiol (—SH) groups on the surface and dispersed in the PSF or cellulose acetate polymer matrix for silver capturing. It was observed that the silver–thiol interaction allows selective silver capture from aqueous solution effectively.[15] The ion-selective nature of nanoclays also makes them a promising choice for the preparation of ion exchange membranes for water applications.[9]

In this study, PSF/PEI nanocomposite membranes were fabricated by blending TEOS for the functionalization of Na-bentonite into the membrane matrix using phase inversion method. The effects of silane-functionalized Na-bentonite and pure Na-bentonite at different concentrations (0.5, 1, and 2 wt%) on the hydrophilicity, permeability, rejection of methylene blue dye, flux recovery ratio (FRR), and DR of PSF/PEI nanocomposite membranes were investigated. The newly prepared silane-functionalized Na-bentonite PSF/PEI nanocomposite membranes were characterized using by Fourier transform infrared spectroscopy (FTIR), scanning electron microscopy (SEM), and atomic force microscopy (AFM). Methylene blue was used as a model organic pollutant to evaluate the rejection performance of the nanocomposite membranes. To the best of our knowledge, there is no documentation of the use of silane-functionalized Na-bentonite in PSF/PEI composite membrane for the rejection of dye from water.

2 | EXPERIMENTAL

2.1 | Materials

Hydrophilic nanoclay (Na-bentonite) fine powder (particle size ≤25 μm) was purchased from Sigma-Aldrich. Polysulfone (PSF) (with average molecular weight [M_w] of 60,000 Da) was used as the polymer in the dope solution (Acros Organics). Branched polyethylenimine (PEI) aqueous solution (with average M_W: 25,000 Da); methylene blue solution (M_w: 319.85); and tetraethoxysilane (TEOS, 97%) were purchased from Sigma-Aldrich. *N*,*N*-dimethylformamide (DMF, anhydrous, 99.8%, Merck) and 1-methyl-2-pyrrolidinone (NMP, Merck) were used as solvents to prepare the membrane cast solution. All chemicals used in the experiments were of reagent grade. The deionized (DI) water was produced by a Milli-Q8 system (Merck Millipore) and used in the sample preparation and for water flux experiments.

2.2 | Methods

2.2.1 | Synthesis of TEOS/Na-bentonite

For synthesis of TEOS/Na-bentonite, 10 g of Na-bentonite powder was weighed and dissolved in 50 ml of acetone until a homogenous mixture was obtained. Then, 2 ml of TEOS was added to the mixture and stirred on magnetic stirrer. It was then heated and mixed rigorously at 50°C for 24 hr.

Finally, the suspension was filtered under vacuum to separate the liquid phase from the functionalized Na-bentonite. The typical synthesis procedure applied for silane functionalized Na-bentonite is schematically presented in Figure 1. As seen in figure, the silane (TEOS) anchored onto Na-bentonite surfaces through condensation reaction between the hydroxyls in hydrolyzed silane and silanol groups on clay mineral surfaces.

2.2.2 | Membrane fabrication

All prepared membranes were fabricated via common phase inversion method as described by Saki and Uzal.[16] The casting solution was made up of PSF (18 wt%), PEI (1 wt%), and different concentrations of pure Na-bentonite and silane-functionalized Na-bentonite (0.5, 1, and 2 wt%). The final solution was mixed for 24 hr at 400 rpm until it became homogeneous. The composition of the casting solutions is detailed in Table 1. The polymer suspension was sonicated for at least 2 hr. All casting solutions were allowed to stand for 1 hr to remove air bubbles. The casting solution was casted onto a clean glass plate with a steel casting knife at a thickness of 110 ± 10 μm. The casted film was immediately immersed in a coagulation bath (DI water at 25°C) for 2 min to remove the residual solvents and complete the phase separation. All prepared membranes were stored in a bottle of DI water at 4°C for characterization and experiments.

2.3 | Characterization of nanoparticles and membranes

2.3.1 | Nanoparticle characterization

Zeta potential measurements were carried out with Nano ZS90 (Malvern, UK) equipment. It automatically calculates the electrophoretic mobility of particles and converts it to the zeta potential.

A total of 0.1 g of sample (TEOS/bentonite/acetone) was conditioned in 100 ml of DI water for 15 min (0.1% solid ratio). The pH of the suspension was adjusted with 0.1 mol/L HCl and 0.1 mol/L NaOH. Then, the suspension was kept for 15 min to allow the larger particles to settle.

Fourier transform infrared spectroscopy (FTIR) was used to characterize the structure of the pure and silane-functionalized Na-bentonite; the methodology used is described in detail in Section 2.3.2.

2.3.2 | Membrane characterization

Scanning electron microscopy

The top-surface and cross-section morphologies of the membranes were evaluated using a scanning electron microscopy (SEM) (Zeiss Evo LS10) with an applied voltage of 10 kV. The membrane samples were fixed at an approximate size of 3 mm length and 0.5 mm width, and then coated with platinum to provide the electrical conductivity.

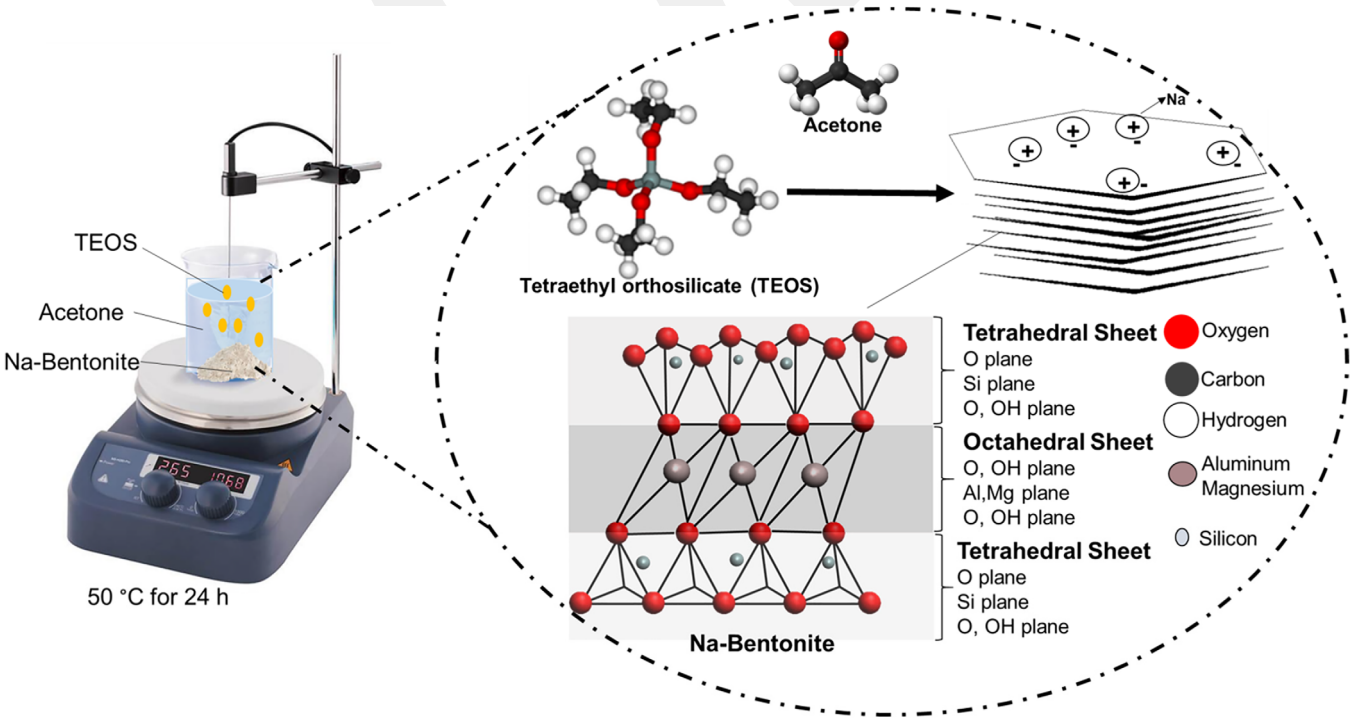

FIGURE 1 Schematic illustration for the synthesis of silane functionalized Na-bentonite [Color figure can be viewed at wileyonlinelibrary.com]

TABLE 1 Casting solution compositions of membranes

Substrate	PSF (wt%)	PEI (wt%)	Na-bentonite (wt%)	Silane-functionalized Na-bentonite (wt%)
PSF	18	—	—	—
PSF/PEI	18	1	—	—
B05	18	1	0.5	—
B1	18	1	1	—
B2	18	1	2	—
SB05	18	1	—	0.5
SB1	18	1	—	1
SB2	18	1	—	2

Abbreviations: PEI, polyethylenimine; PSF, polysulfone.

Atomic force microscopy

AFM was used to analyze all prepared membranes via a MultiMode 8-HR, Veeco microscope operated in tapping mode (Model: RTESP-300). Each membrane was dried overnight at 80°C. The analysis was conducted to scan the membrane surface in an area of 5×5 μm^2. The roughness parameters calculated in terms of average roughness (R_a), root mean square roughness (R_q) and maximum difference in height between the highest and lowest point (R_{max}) were reported as the average of at least two analyses on the membranes.

Fourier transform infrared spectroscopy

FTIR spectra were employed for functional identification of PEI, Na-bentonite, and silane-functionalized Na-bentonite on the polymer backbone in the composite blend membranes by using an FTIR spectrometer (Thermo Nicolet Avatar 370) in the wave number range from 4,000 to 400 cm^{-1}. The samples were dried in an oven for 15 min at 120°C.

Contact angle

The surface hydrophilicity of the membranes was measured through the sessile drop method using a contact angle meter (Attention-Theta Lite, Biolin Scientific, Finland). DI water was used as the probe liquid to compare the hydrophilicity of membranes, and the measurement was conducted by dropping 3 μl DI water on the membrane surface at 25°C. An average value was obtained from three random locations for each membrane. All of the membranes were fully dried before measuring the contact angle to avoid issues with water interaction.

Porosity

The bulk porosity (ε %) of the membranes was found by the gravimetric method. To obtain the porosity, dry membrane was dipped in water for 24 hr and then carefully removed and swiped with filter paper to remove excess water prior to weighing. Afterward, the membranes were dried in an oven at 50°C for 24 hr and weighed again. The thicknesses of dried membrane were measured with an electronic micrometer device of ±0.1 μm precision (Mitutoyo, Japan). To correlate the results, measurements were repeated twice, as specified in the following equation:

$$\text{Porosity}\,(\%) = \frac{\text{Ww} - \text{Wd}}{\rho \text{Al}} \times 100 \quad (1)$$

where W_w and W_d are wet and dry membrane weights (g); and ρ, A, and l are the water density (g/cm^3), membrane effective area (m^2), and thickness (m), respectively.

2.3.3 | Water filtration and methylene blue rejection tests

Filtration tests were carried out in batch scale, in a dead-end stirred cell filtration system (Sterlitech, HP4750) with an effective membrane surface area of 14.6 cm^2 and a volume capacity of 300 ml. Membrane filtration cell was connected with a nitrogen gas cylinder. The pure water flux was determined at constant transmembrane pressure of 2 bar. The membrane was then compressed at 2.5 bar to achieve steady permeate and the pure water flux was recorded every 15 min. The water fluxes of the prepared membranes were calculated using Equation (2):

$$J = \frac{V}{A \times t} \quad (2)$$

where J is the water flux (L m^{-2} h^{-1}), V is the permeate volume (L), A is the effective membrane area (m^2), and t is the time (h).

The dye rejection efficiency of the membranes was evaluated using methylene blue as a model pollutant at room temperature. For this purpose, the stirred cell reservoir was refilled with methylene blue at a concentration of 50 ppm and stirring speed of 400 rpm at room temperature

(25 ± 5°C). The flux for methylene blue, J_1 (L m^{-2} h^{-1}), was measured based on the pure water flux calculation. Methylene blue concentrations were analyzed using ultraviolet–visible spectroscopy (UV-DR-6000; Shimadzu, China) at a wavelength of 663 nm. The methylene blue rejection (R) was calculated by Equation (3):

$$\%R = 1 - \frac{Cp}{Cf} \times 100 \quad (3)$$

where C_p is the concentration of methylene blue in the permeate, and C_f is the concentration of methylene blue in the feed solution.

After the filtration of methylene blue, the membranes were cleaned with DI water for 20 min, then the DI water flux of cleaned membranes J_2 (L m^{-2} h^{-1}) was measured again. Fouling resistance, including flux decay ratio (DR) and FRR, was calculated using the following equations[17,18]:

$$DR = \frac{J - J1}{J} \times 100 \quad (4)$$

$$FRR = \frac{J2}{J1} \times 100 \quad (5)$$

The lower DR and higher FRR values proves the better antifouling capacity of the membranes in filtration applications.[19]

3 | RESULTS AND DISCUSSION

3.1 | Modification of Na-bentonite

3.1.1 | Zeta potential measurements

Zeta potential measurements revealed the electrokinetic behaviors of pure Na-bentonite and TEOS-functionalized Na-bentonite samples.[20] As seen from Figure 2, pure bentonite has negative zeta potential values within the pH range (5 ≤ pH ≤11.3) and the surface negativity increases with increasing pH, which is in accordance with literature.[21–23] TEOS functionalization of Na-bentonite samples (1, 2, and 5%wt) shifts the zeta potential values to more negative values because the silane coupling agent acts as the hydrophilic layer.[24]

3.1.2 | Fourier transform infrared spectroscopy

The FTIR spectra of pure and silane Na-bentonite samples (in Figure 3) were measured in transmittance

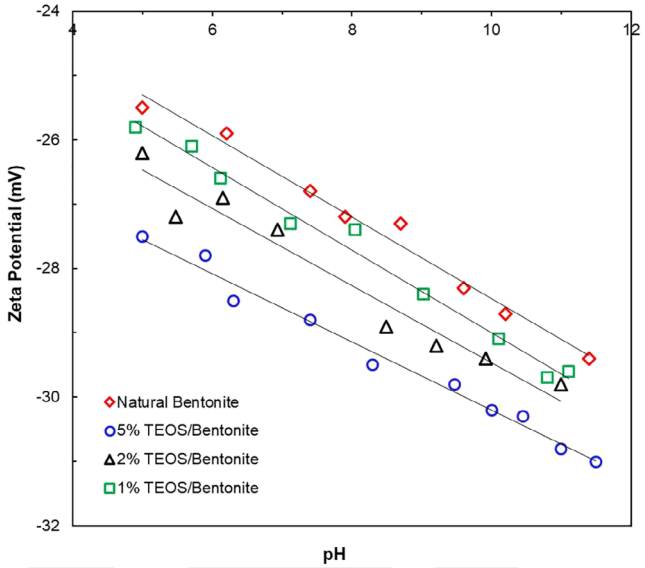

FIGURE 2 Zeta potential of tetraethoxysilane (TEOS)/Na-bentonite/acetone sample [Color figure can be viewed at wileyonlinelibrary.com]

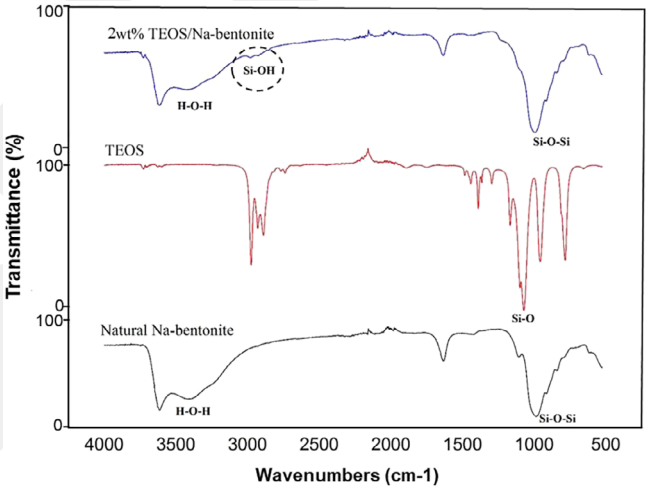

FIGURE 3 Fourier transform infrared spectroscopy (FTIR) spectra of natural Na-bentonite, tetraethoxysilane (TEOS), and 2 wt % TEOS/Na-bentonite [Color figure can be viewed at wileyonlinelibrary.com]

(mixture of 1 mg samples with 100 mg KBr). The bands at 463 and 518 cm^{-1} are due to Si—O—Si and Al—O—Si bending vibrations, respectively.[25] The first strong adsorption band observed at about 1,050 cm^{-1} can be attributed to Si—O—Si groups stretching vibration. The bands at 3,500 cm^{-1} are attributable to OH (hydroxyl) vibrations of the H—O—H group which interlayer water molecules on Na-bentonite.[26,27]

As seen from Figure 3, the bands are present at 2,700–3,000 cm^{-1} which correspond to Si—OH bending

vibrations. The peak at 3,650 cm^{-1} is related to Si—OH stretching vibration. These bands are strong evidence of silane (TEOS)-functionalization of Na-bentonite.[28]

3.2 | Membrane characterization

3.2.1 | SEM images

SEM images were taken to examine the effect of PEI, Na-bentonite and silane-functionalized Na-bentonite on the top and cross section of PSF-based membrane morphologies. SEM was used to understand the structural changes in PSF matrix incorporated with PEI. Figure 4 shows SEM images of the top surfaces and cross sections of PSF and PSF/PEI composite membranes. PSF of 18 wt % has a standard surface without any pores, the surface pore structure was visually changed and a new porous structure was created with the addition of 1 wt% PEI to the polymer matrix. It was recently reported that the thermodynamic exchange of membrane casting solution during the coagulation process was improved by adding hydrophilic PEI; consequently, rapid phase remixing was encouraged and then large pores were created.[29]

Surface and cross-sectional images of the PSF/PEI membranes with different concentrations of Na-bentonite (0.5, 1, and 2 wt%) are shown in Figure 5. As seen from the figure, Na-bentonite concentration was 2 wt%; no agglomeration problem was observed on membrane surface. In addition, the cross sections of the PSF/PEI/1 wt% Na-bentonite membranes exhibited small finger-like structures which were likely due to the improved diffusion ratio of the membrane solution. This can be attributed to the hydrophilic nature of Na-bentonite.[30]

Figure 6 shows the top and cross-sectional SEM micrograph of the prepared silane-functionalized Na-bentonite PSF/PEI nanocomposite membranes, which exhibited new morphological changes in the nanocomposite membrane. It is clearly seen in Figure 6 that the finger-like structure and membrane porosity increased with the incorporation of silane-functionalized Na-bentonite in the membrane matrix. The addition of

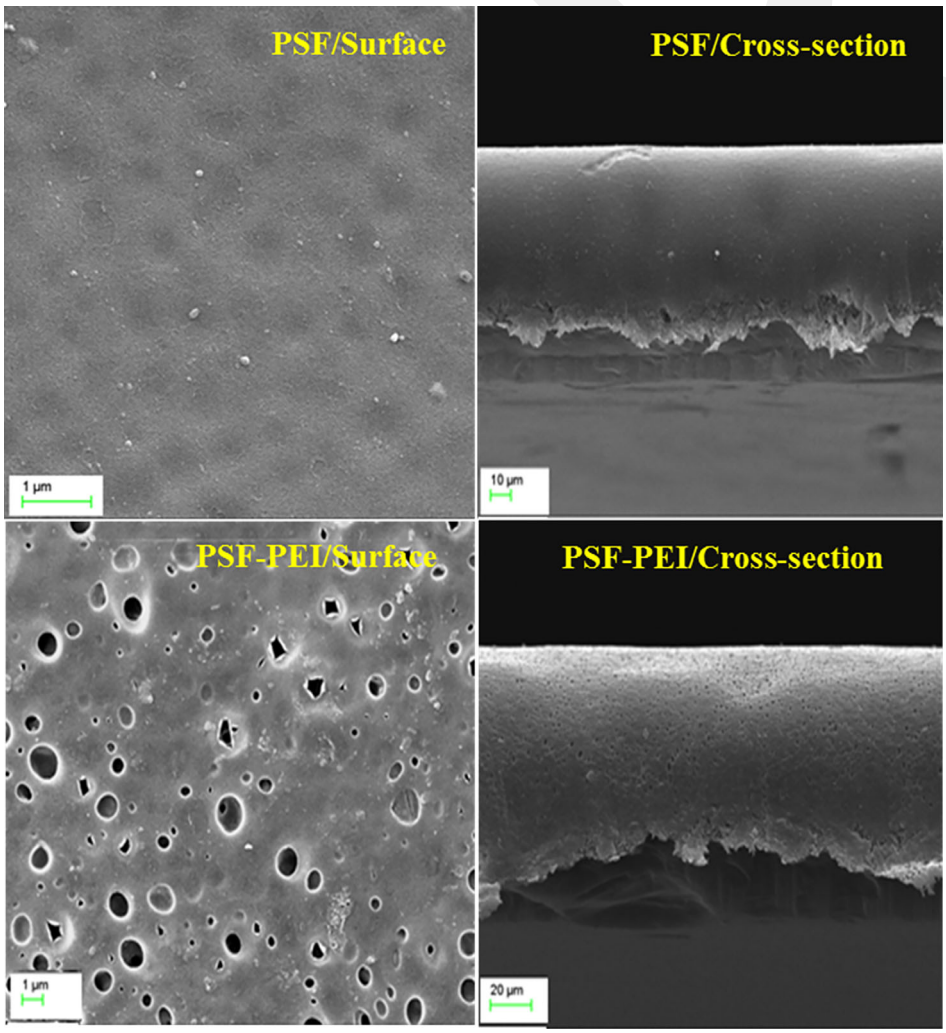

FIGURE 4 Cross section and surface scanning electron microscopy (SEM) images of polysulfone (PSF) and PSF/polyethylenimine (PEI) membranes [Color figure can be viewed at wileyonlinelibrary.com]

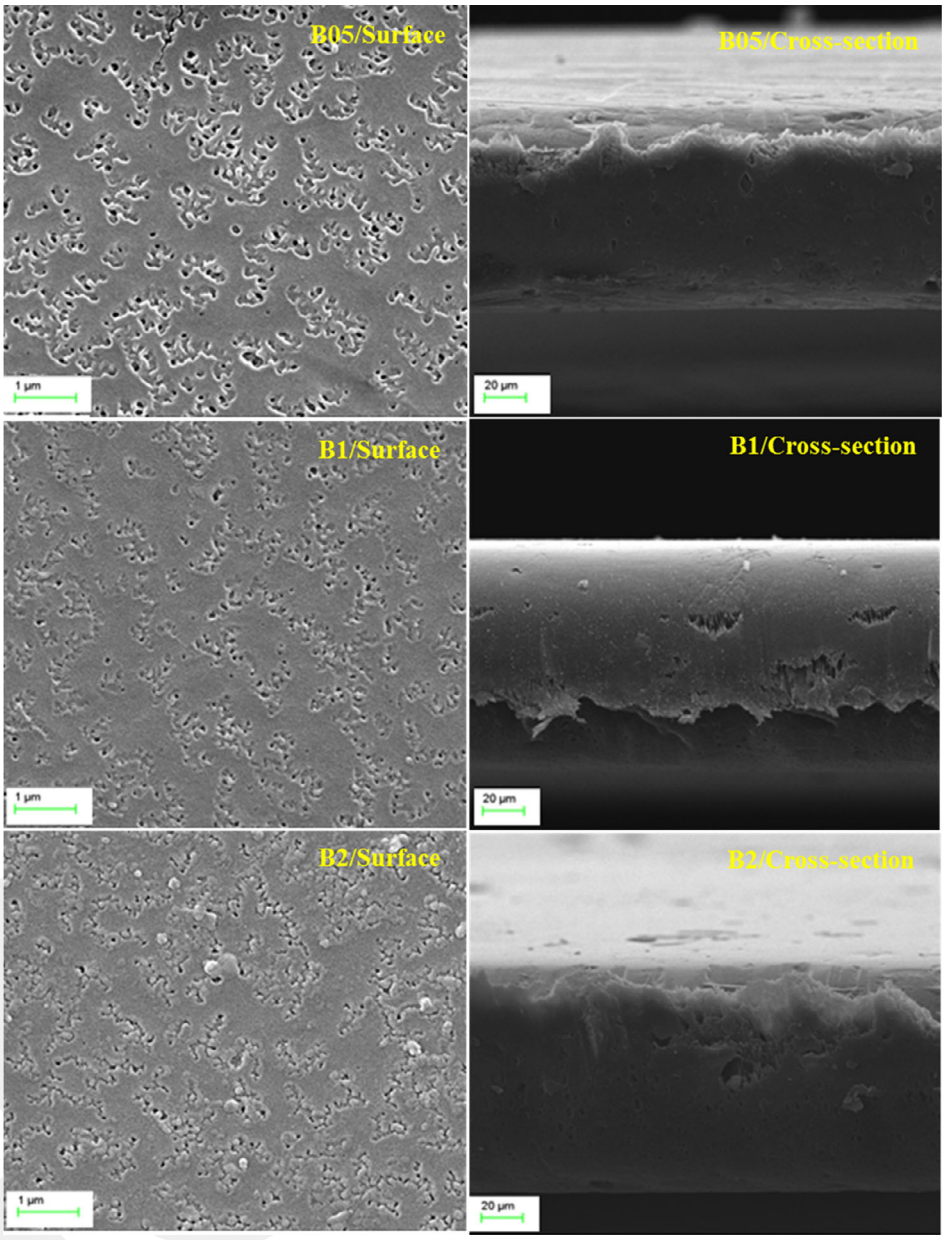

FIGURE 5 Cross section and surface scanning electron microscopy (SEM) images of polysulfone/polyethylenimine (PSF/PEI) nanocomposite membranes containing Na-bentonite [Color figure can be viewed at wileyonlinelibrary.com]

hydrophilic, modified silane-functionalized Na-bentonite enhanced the hydrophilicity of PSF/PEI casting solution, which encouraged the fast exchange between DMF/NMP and DI water, thereby increasing the number of pores and in accordance with literature.[13]

3.2.2 | AFM analysis

To investigate the topography of fabricated membranes, AFM images were taken at a scanning area of $5 \times 5\ \mu m^2$. The three-dimensional AFM images of PSF and PSF/PEI membranes are shown in Figure 7. Although peak-to-valley morphology was observed for pure PSF, blending of hydrophilic PEI caused uniform nodule distribution. Consequently, the average roughness (R_a) of the PSF membrane was reduced from 24 to 15 nm with PEI addition.

The three-dimensional images of the nanocomposite membranes containing natural and silane-functionalized Na-bentonite samples obtained by AFM studies are presented in Figure 8. All AFM images showed different topographies at various levels. The surface of B05, B1, and B2 nanocomposite membranes showed irregular edges, well-defined hills and a number of depressions, suggesting a surface with great roughness. On the other hand, interfacial crosslinking reaction successfully obtained with surface modification of Na-bentonite.[31] The same behavior of roughness reduction was reported by Vatanpour et al. where boehmite nanoparticles served

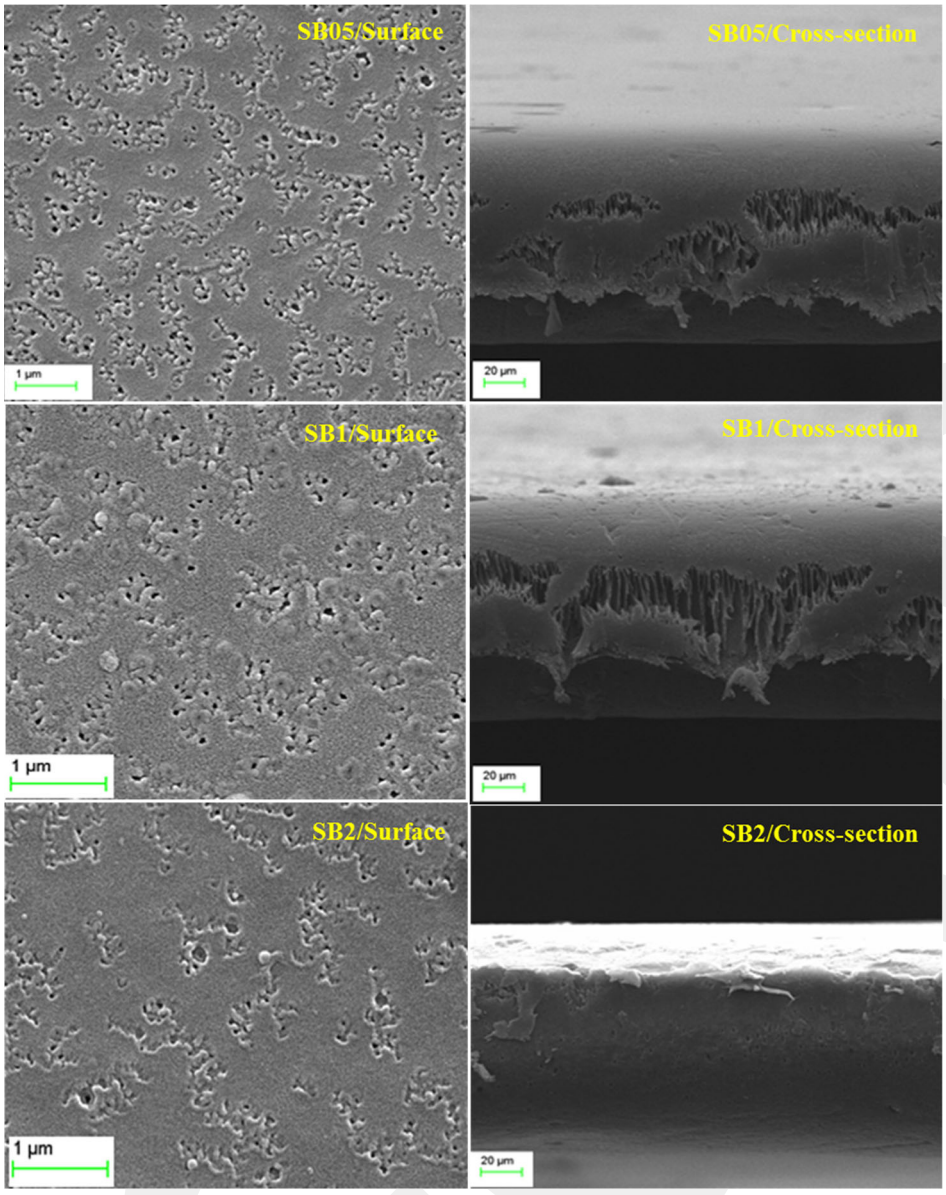

FIGURE 6 Cross-section and surface scanning electron microscopy (SEM) images of polysulfone/polyethylenimine (PSF/PEI) nanocomposite membranes containing silane-functionalized Na-bentonite [Color figure can be viewed at wileyonlinelibrary.com]

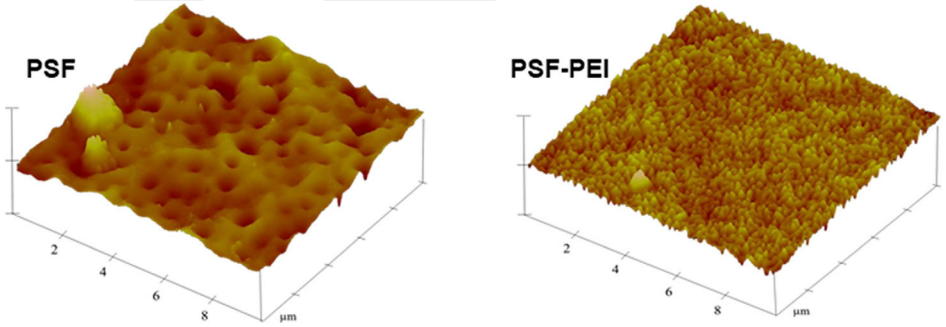

FIGURE 7 Atomic force microscopy (AFM) images of polysulfone (PSF) and PSF/polyethylenimine (PEI) membranes [Color figure can be viewed at wileyonlinelibrary.com]

as advance nanofiller for the preparation of polyethersulfone nanocomposite membranes.[32]

The roughness parameters, R_q, R_a, and R_{max} are given in Table 2. Silane-functionalized Na-bentonite nanocomposite membrane showed lower surface roughness when compared to the natural Na-bentonite nanocomposite membrane. SB2 membrane showed the lowest R_a value of 12 nm. This clearly indicates that silane-functionalized Na-bentonite particles were effectively distributed on the membrane surface and filled the nodules structures of the

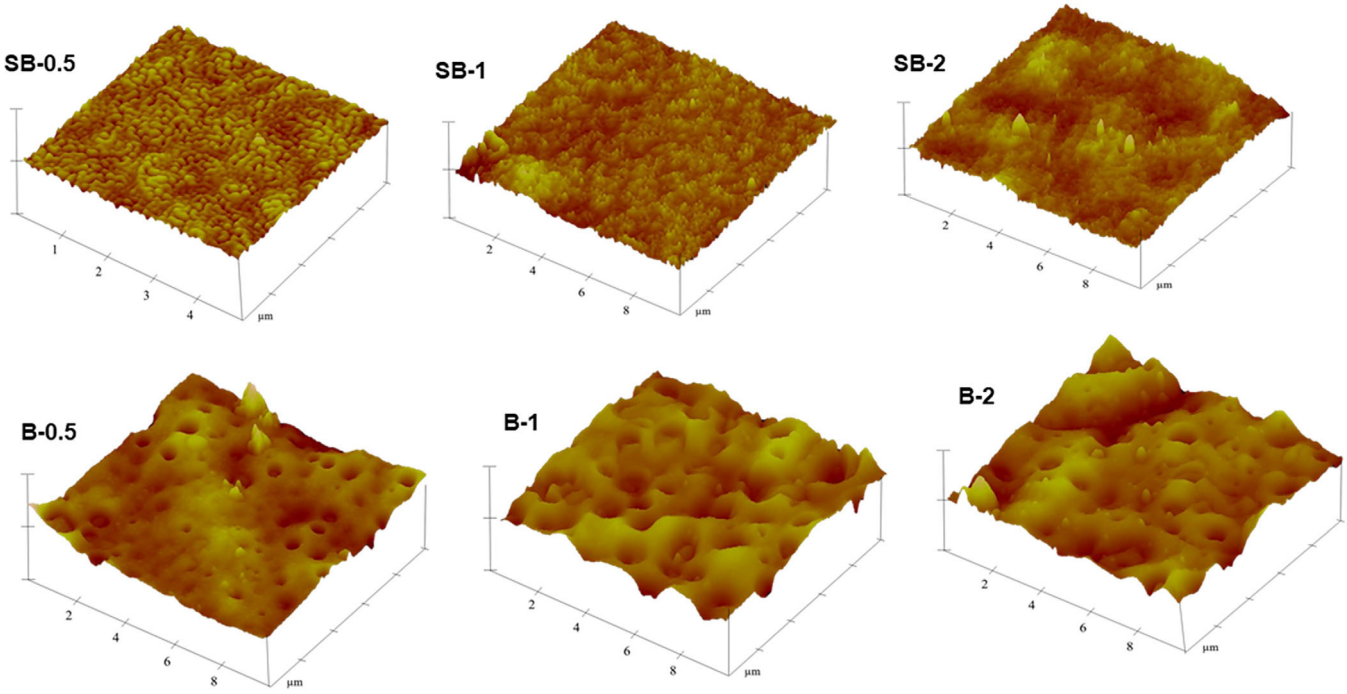

FIGURE 8 Atomic force microscopy (AFM) images polysulfone/polyethylenimine (PSF/PEI) nanocomposite membranes containing pure Na-bentonite and silane functionalized Na-bentonite [Color figure can be viewed at wileyonlinelibrary.com]

TABLE 2 Surface roughness parameters of PSF, PSF/PEI, and nanocomposite membranes

Substrate	R_q (nm)	R_a (nm)	R_{max} (nm)
PSF	33 ± 3.0	24 ± 2.1	403 ± 32.5
PSF/PEI	18 ± 1.5	15 ± 1.1	170 ± 15.6
B05	25 ± 2.0	19 ± 1.2	266 ± 24.8
B1	44 ± 3.2	35 ± 3.3	329 ± 31.2
B2	35 ± 3.1	27 ± 2.5	325 ± 30.7
SB05	16 ± 1.5	12 ± 1.0	193 ± 17.9
SB1	27 ± 2.5	21 ± 1.9	335 ± 8.5
SB2	15 ± 0.8	12 ± 0.9	159 ± 11.5

Abbreviations: PEI, polyethylenimine; PSF, polysulfone.

membrane surface.[33] It is known that lower membrane roughness and surface energy results in stronger antifouling capacity.[34] These results along with the following dye rejection experiments support the use of modified Na-bentonite as a new approach for making membrane with improved antifouling ability.

3.2.3 | Membrane porosity and hydrophilicity

Membrane porosity is one of the crucial factors that affect the permeability behavior of prepared membranes. Na-bentonite was well dispersed with different ratios in fabricated membrane structure and porous Na-bentonite in PSF polymer matrix demonstrates higher porosity that is very promising for water treatment applications. Consequently, the pore formation process would be improved in PSF/PEI membrane matrix incorporation with silane-functionalized Na-bentonite. It can be seen from Table 3 that porosity values were significantly higher with natural and silane-functionalized Na-bentonite loading when compared to the PSF and PSF/PEI membranes. This can be explained on the basis of the high hydrophilic characteristic of Na-bentonite in the PSF matrix, which increased the formation of large pores on the membrane structure.

The hydrophilicity of PSF, PSF/PEI, and nanocomposite membranes were measured and the results obtained are presented in Table 3. Contact angle of pristine PSF was 93° due to the intrinsic hydrophobic characteristics of the polymer. However, the contact angle of nanocomposite membranes was decreased significantly by blending with different concentrations of natural and silane-functionalized Na-bentonite. While PSF/PEI/2 wt% Na-bentonite had the highest water contact angle (81°), PSF/PEI/0.5 wt% Na-bentonite had lower contact angle (69°). The increased hydrophilicity of the nanocomposite membranes can be attributed to the presence of hydrophilic Na-bentonite consisting of hydroxyl functional groups on their surface, thus changing the interfacial free energy at the membrane surface in the

TABLE 3 Porosity, contact angle, and pure water flux (2 bar) and of PSF, PSF/PEI, and natural and silane functionalized Na-bentonite nanocomposite membrane

Substrate	Porosity (%)	Contact angle (°)	Flux (L m^{-2} h^{-1})
PSF	18 ± 0.3	93 ± 2.8	1.2 ± 0.1
PSF/PEI	55 ± 1.6	70 ± 5.1	115 ± 4.8
B05	62 ± 2.7	69 ± 3.0	41 ± 1.0
B1	72 ± 2.4	75 ± 2.6	53 ± 1.2
B2	76 ± 2.2	81 ± 0.9	70 ± 2.3
SB05	65 ± 1.9	73 ± 1.4	50 ± 0.7
SB1	74 ± 3.1	79 ± 0.7	66 ± 1.3
SB2	82 ± 2.9	80 ± 1.0	105 ± 3.4

Abbreviations: PEI, polyethylenimine; PSF, polysulfone.

TABLE 4 Methylene blue rejection ratio (%), FRR (%) and DR (%) values to PSF, PSF/PEI, and natural and silane functionalized Na-bentonite nanocomposite membranes

Substrate	Methylene blue rejection (%)	DR (%)	FRR (%)
PSF	93.6	65	78
PSF/PEI	94.2	72	73
B05	96.7	42	86
B1	95.4	44	87
B2	95.2	39	89
SB05	98.6	30	92
SB1	98.2	11	95
SB2	98.9	12	93

Abbreviations: DR, decay ratio; FRR, flux recovery ratio; PEI, polyethylenimine; PSF, polysulfone.

coagulation bath.[35] Similarly, Farahani and Vatanpour prepared PVDF membrane incorporated with nanoclay, resulting in small changes in water contact angle; these minor changes may be attributed to the amphipathic characteristics of nanoclay.[7]

3.2.4 | Water filtration and methylene blue rejection experiments

Filtration experiments were conducted to study the permeability of PSF/PEI membranes with different contents of natural and silane-functionalized Na-bentonite. The water fluxes of the membranes were determined at 2 bar by using dead-end filtration and the results are given in Table 3. The natural PSF membrane exhibited the lowest water flux of 1.2 L m^{-2} h^{-1}, and the highest water flux was obtained for the membranes with 2 wt% silane-functionalized Na-bentonite as 105 L m^{-2} h^{-1}. The pure water flux of the SB2 nanocomposite membrane improved over 98 times higher than natural PSF membrane. This result could be explained by the improvement of the hydrophilicity and porosity of nanocomposite membranes by the addition of silane-functionalized Na-bentonite.[36,37] The incorporation of natural and silane-functionalized Na-bentonite leads to a more porous structure as observed from the SEM images, which decreased the water permeation resistance through the membranes. Moreover, nanocomposite membranes tend to absorb water molecules better than pristine PSF because of enhanced hydrophilicity that means higher water permeability.[38] Silane-modified clays are useful adsorbents because of their marked ability in removing pollutants such as dyes and inorganic cations from solution. Queiroga et al. used the amino-modified bentonite solids to remove Reactive Violet 5R from aqueous solutions and reported higher functionalization degrees with nonpolar solvents containing organobentonite.[39]

Methylene blue dye rejection experiments were performed to test the antifouling behavior of fabricated nanocomposite membranes. For the antifouling tests, the feed concentration plays a critical role in separation performance. Thus, dye removal experiments were carried out at three different dye concentrations (20, 50, and 100 ppm). The highest dye rejection, expressed as a percentage, was obtained for 50 ppm concentration of methylene blue dye. The FRR, DR, and methylene blue rejection ratio for PSF, PSF/PEI, and nanocomposite membranes are given in Table 4. For the rejection of dyes from water, the separation depends not only on the pore size but also on the effect of the electrostatic interaction between the membrane surface and the dye molecules.[40] Methylene blue dye rejection ratio (Table 4) increased from 93.6 to 98.6%, 98.2%, and 98.9% when 0.5, 1, and 2 wt% silane-functionalized Na-bentonite were added to the PSF casting solution, respectively. It is known that Na-bentonite surface has a strong negative charge in neutral pH value.[41] The newly fabricated nanocomposite membranes had negatively charged surface with the addition of silane-functionalized Na-bentonite, which effectively rejected the negative dye molecules and led to higher dye removal.[42]

Hydrophobic materials such as PSF need to be improved for their antifouling characteristics which affects the filtration efficiency. The addition of negatively charged natural and silane-functionalized Na-bentonite can sufficiently reduce the interaction between methylene blue and membrane surface, thus improving antifouling resistance. All nanocomposite membranes showed superior antifouling properties compared with the natural PSF membrane with higher FRR values. From Table 4, comparing FRR of the prepared membranes with blending natural and

silane-functionalized Na-bentonite revealed that silane-functionalized Na-bentonite in the membrane matrix led to the improvement of the antifouling characteristic of the prepared novel nanocomposite membrane. FRR increased to the highest value of 95% as the silane-functionalized Na-bentonite loading increased to 1%. These results are in good agreement with the nanocomposite membrane incorporated with nanoparticle for water treatment applications.[43]

4 | CONCLUSIONS

In the present work, Na-bentonite was modified with TEOS and incorporated into PSF/PEI polymer mixture to prepare nanocomposite membranes with improved water permeability and antifouling capacity. The main conclusions were summarized as follows:

1. The characterizations of silane-functionalized Na-bentonite PSF/PEI nanocomposite membranes indicated that the binding between Na-bentonite and TEOS was successful with the support of functional groups, finger-like structures, and lower surface roughness confirmed by FTIR, SEM, and AFM measurements, respectively.
2. The hydrophilicity of PSF/PEI nanocomposite membranes were significantly improved by the incorporation of natural and silane-functionalized Na-bentonite, which providing hydrophilic functional groups, and 0.5 wt% Na-bentonite nanocomposite membrane exhibited the lowest contact angle of 69.
3. The addition of natural and silane-functionalized Na-bentonite in the membrane matrix increased water permeability. The maximum water flux of 105 L m^{-2} h^{-1} was obtained for 2 wt% silane-functionalized Na-bentonite PSF/PEI membranes s while the lowest water flux (1.2 L m^{-2} h^{-1}) was recorded for natural PSF membrane.
4. The prepared silane-functionalized Na-bentonite PSF/PEI nanocomposite membrane presented superior antifouling property for methylene dye rejection, which is mainly attributed to its special negatively charged silane surface. Based on the results, among the membranes fabricated, the PSF/PEI membrane containing 1 wt% silane functionalized Na-bentonite showed the best performance with nearly 100% methylene blue rejection, 11% DR and 95% FRR.

Silane-functionalized Na-bentonite PSF/PEI nanocomposite membranes have potential application in the treatment of dye-contaminated waters, especially in the textile sector. In further studies, we will continue to explore the performance of this membrane in a wide range of wastewater treatment applications.

ORCID

Nigmet Uzal https://orcid.org/0000-0002-0912-3459

REFERENCES

[1] A. Bouazizi, S. Saja, B. Achiou, M. Ouammou, J. Calvo, A. Aaddane, S. A. Younssi, *Appl. Clay Sci.* **2016**, *132*, 33.
[2] C.-Y. Wang, W.-J. Zeng, T.-T. Jiang, X. Chen, X.-L. Zhang, *Sep. Purif. Technol.* **2019**, *214*, 21.
[3] E. Sahinkaya, A. Yurtsever, Ö. Çınar, *Sep. Purif. Technol.* **2017**, *174*, 445.
[4] Robert. D. Crangle, Jr., *U.S. Geological Survey Minerals Yearbook*, United States Government Publishing Office, Eastern Region Reston Va **2016**.
[5] Y. K. Ong, F. Y. Li, S.-P. Sun, B.-W. Zhao, C.-Z. Liang, T.-S. Chung, *Chem. Eng. Sci.* **2014**, *114*, 51.
[6] D. S. Dlamini, J. Li, B. B. Mamba, *Appl. Clay Sci.* **2019**, *168*, 21.
[7] M. H. D. A. Farahani, V. Vatanpour, *Sep. Purif. Technol.* **2018**, *197*, 372.
[8] G. Zeng, Z. Ye, Y. He, X. Yang, J. Ma, H. Shi, Z. Feng, *Chem. Eng. J.* **2017**, *323*, 572.
[9] F. Radmanesh, T. Rijnaarts, A. Moheb, M. Sadeghi, W. M. De Vos, *J. Colloid Interface Sci.* **2019**, *533*, 658.
[10] E. Koksal, B. Afsin, A. Tabak, B. Caglar, *Spectrosc. Lett.* **2011**, *44*, 77.
[11] S. Nivedita, S. Joseph, *J. Water Process Eng.* **2018**, *21*, 61.
[12] S. Yang, D. Zhao, H. Zhang, S. Lu, L. Chen, X. Yu, *J. Hazard. Mater.* **2010**, *183*, 632.
[13] G. Zeng, Y. He, Y. Zhan, L. Zhang, Y. Pan, C. Zhang, Z. Yu, *J. Hazard. Mater.* **2016**, *317*, 60.
[14] Z. Xu, J. Zhang, M. Shan, Y. Li, B. Li, J. Niu, B. Zhou, X. Qian, *J. Membr. Sci.* **2014**, *458*, 1.
[15] A. Ladhe, P. Frailie, D. Hua, M. Darsillo, D. Bhattacharyya, *J. Membr. Sci.* **2009**, *326*, 460.
[16] S. Saki, N. Uzal, *Environ. Sci. Pollut. Res.* **2018**, *25*, 25315.
[17] W. Chen, Y. Su, L. Zheng, L. Wang, Z. Jiang, *J. Membr. Sci.* **2009**, *337*, 98.
[18] S. Zhao, Z. Wang, X. Wei, B. Zhao, J. Wang, S. Yang, S. Wang, *J. Membr. Sci.* **2011**, *385*, 251.
[19] L. Wang, Y.-L. Su, L. Zheng, W. Chen, Z. Jiang, *J. Membr. Sci.* **2009**, *340*, 164.
[20] R. J. Hunter, *Zeta Potential in Colloid Science: Principles and Applications*, Academic Press, San Diego, CA **2013**.
[21] M. Abdel-Khalek, H. Ahmed, A. El-Midany, *J. Ore Dressing* **2015**, *17*, 11.
[22] W. Mekhamer, *J. Saudi Chem. Soc.* **2010**, *14*, 301.
[23] P.-I. Au, Y.-K. Leong, *KONA Powder Part. J.* **2016**, *33*, 17.
[24] H. Yan, W. Yuanhao, Y. Hongxing, *Appl. Energy* **2017**, *185*, 2209.
[25] H. Zaitan, D. Bianchi, O. Achak, T. Chafik, *J. Hazard. Mater.* **2008**, *153*, 852.
[26] L. Zhirong, M. A. Uddin, S. Zhanxue, *Spectrochim. Acta B* **2011**, *79*, 1013.
[27] Z. Mičicová, S. Božeková, M. Pajtášová, D. Ondrušová, *MATEC Web Conf.* **2018**, *157*, 07006.
[28] N. Guermat, A. Bellel, S. Sahli, Y. Segui, P. Raynaud, *M. J. Condens. Mater.* **2010**, *12*, 208.
[29] V. Vatanpour, S. S. Madaeni, R. Moradian, S. Zinadini, B. Astinchap, *Sep. Purif. Technol.* **2012**, *90*, 69.
[30] M. Kumar, M. Ulbricht, *J. Membr. Sci.* **2013**, *448*, 62.

[31] M. Peyravi, M. Jahanshahi, A. Rahimpour, A. Javadi, S. Hajavi, *Chem. Eng. J.* **2014**, *241*, 155.
[32] V. Vatanpour, S. S. Madaeni, L. Rajabi, S. Zinadini, A. A. Derakhshan, *J. Membr. Sci.* **2012**, *401*, 132.
[33] B. Rajaeian, A. Rahimpour, M. O. Tade, S. Liu, *Desalination* **2013**, *313*, 176.
[34] A. Razmjou, J. Mansouri, V. Chen, *J. Membr. Sci.* **2011**, *378*, 73.
[35] Z. G. Cui, K. Z. Shi, Y. Z. Cui, B. P. Binks, *Colloids Surf. A: Physicochem. Eng. Asp.* **2008**, *329*, 67.
[36] E. Celik, L. Liu, H. Choi, *Water Res.* **2011**, *45*, 5287.
[37] E.-S. Kim, G. Hwang, M. Gamal El-Din, Y. Liu, *J. Membr. Sci.* **2012**, *394–395*, 37.
[38] E. Yuliwati, A. Ismail, *Desalination* **2011**, *273*, 226.
[39] L. N. Queiroga, M. B. Pereira, L. S. Silva, E. C. Silva Filho, I. M. Santos, M. G. Fonseca, T. Georgelin, M. Jaber, *Appl. Clay Sci.* **2019**, *168*, 478.
[40] L. Shao, X. Q. Cheng, Y. Liu, S. Quan, J. Ma, S. Z. Zhao, K. Y. Wang, *J. Membr. Sci.* **2013**, *430*, 96.
[41] J. Zhu, N. Guo, Y. Zhang, L. Yu, J. Liu, *J. Membr. Sci.* **2014**, *465*, 91.
[42] V. Gupta, *J. Environ. Manag.* **2009**, *90*, 2313.
[43] V. Vatanpour, M. Esmaeili, M. H. D. A. Farahani, *J. Membr. Sci.* **2014**, *466*, 70.

How to cite this article: Saki S, Senol-Arslan D, Uzal N. Fabrication and characterization of silane-functionalized Na-bentonite polysulfone/polyethylenimine nanocomposite membranes for dye removal. *J Appl Polym Sci*. 2020;137:e49057. https://doi.org/10.1002/app.49057